HIV-Nef and ADAM17-Containing Plasma Extracellular Vesicles Induce and Correlate with Immune Pathogenesis in Chronic HIV Infection

Jung-Hyun Lee, Stephan Schierer, Katja Blume, Jochen Dindorf, Sebastian Wittki, Wei Xiang, Christian Ostalecki, Nina Koliha, Stefan Wild, Gerold Schuler, Oliver T. Fackler, Kalle Saksela, Thomas Harrer, Andreas S. Baur

PII: S2352-3964(16)30087-1
DOI: doi: 10.1016/j.ebiom.2016.03.004
Reference: EBIOM 508

To appear in: *EBioMedicine*

Received date: 27 December 2015
Revised date: 19 February 2016
Accepted date: 2 March 2016

Please cite this article as: Lee, Jung-Hyun, Schierer, Stephan, Blume, Katja, Dindorf, Jochen, Wittki, Sebastian, Xiang, Wei, Ostalecki, Christian, Koliha, Nina, Wild, Stefan, Schuler, Gerold, Fackler, Oliver T., Saksela, Kalle, Harrer, Thomas, Baur, Andreas S., HIV-Nef and ADAM17-Containing Plasma Extracellular Vesicles Induce and Correlate with Immune Pathogenesis in Chronic HIV Infection, *EBioMedicine* (2016), doi: 10.1016/j.ebiom.2016.03.004

HIV-Nef and ADAM17-containing plasma extracellular vesicles induce and correlate with immune pathogenesis in chronic HIV infection

Jung-Hyun Lee[1], Stephan Schierer[1], Katja Blume[1], Jochen Dindorf[1], Sebastian Wittki[1], Wei Xiang[2], Christian Ostalecki[1], Nina Koliha[3], Stefan Wild[3], Gerold Schuler[1], Oliver T. Fackler[4], Kalle Saksela[5], Thomas Harrer[6] and Andreas S. Baur[1*]

[1]Department of Dermatology, University Hospital Erlangen, Friedrich-Alexander-University of Erlangen-Nürnberg, Translational Research Center, Ulmenweg 12, 91054 Erlangen, Germany.
[2]Department for Biochemistry and Molecular Medicine, Friedrich-Alexander University of Erlangen-Nürnberg, Fahrstraße 17, 91054 Erlangen, Germany.
[3]Miltenyi Biotec GmbH, Friedrich-Ebert-Straße 68, 51429 Bergisch Gladbach, Germany.
[4] Department of Infectious Diseases, Integrative Virology, University Hospital Heidelberg, Im Neuenheimer Feld 324, 69120 Heidelberg, Germany.
[5]Department of Virology, 00014 University of Helsinki, PO Box 21 (Haartmaninkatu 3), Finland.
[6]Department for Internal Medicine 3, University Hospital Erlangen, Friedrich-Alexander-University of Erlangen-Nürnberg, Ulmenweg 18, 91054 Erlangen.

*Correspondence to: andreas.baur@uk-erlangen.de

Highlights:

-Viremic and non-viremic HIV patients harbor high levels of plasma extracellular vesicles.

-Besides inflammatory factors they contain Nef and Vpu, hinting at ongoing viral activity despite efficient ART.

-The level of Nef vesicles correlate with immunactivation and low CD4 levels in chronic HIV infection.

Research in Context

Lee et al. found high levels of extracellular vesicles in plasma (pEV) in HIV infection that did not decline under treatment and analyzed a possible correlation with HIV pathogenesis. The pEV contained inflammatory factors and HIV proteins. This was unexpected as viral replication is efficiently suppressed by treatment. The pEV content and viral proteins correlated stringently with symptoms of chronic HIV disease, including low T cell count and increased inflammation. Analyzing the cytokine pattern of HIV pEV it seemed that they were secreted by a so far unknown cell compartment. Suppressing pEV secretion may greatly improve the treatment of chronic HIV infection.

Abstract

Antiretroviral therapy (ART) efficiently suppresses HIV replication but immune activation and low CD4 T cell counts often persist. The underlying mechanism of this ART-resistant pathogenesis is not clear. We observed that levels of plasma extracellular vesicles (pEV) are strongly elevated in HIV infection and do not decline during ART. Surprisingly, these vesicles contained the viral accessory proteins Nef and Vpu, which are assumed to be not expressed under efficient ART, as well as pro-inflammatory effectors, including activated ADAM17. HIV pEV were characterized by the presence of activated $\alpha v\beta 3$ and absence of CD81 and Tsg101. Correlating with immune activation, peripheral monocytes ingested large amounts of pEV, giving rise to an increased population of CD1c+CD14+ cells that secreted inflammatory cytokines. Importantly, the pro-inflammatory content, particularly ADAM17 activity, correlated with low T cell counts. Preliminary evidence suggested that HIV pEV derived from peripheral mononuclear cells and from an unknown myeloid cell population. In summary we propose an important role of pro-inflammatory pEV in chronic HIV infection due to ongoing viral Nef activity.

Introduction

HIV is targeting predominantly T cells, most of which are killed rapidly after infection (Perelson et al., 1996; Ho et al., 1995; Doitsh et al., 2014), but leave behind a small reservoir of largely inactive proviruses (Eriksson et al., 2013; Eisele and Siliciano, 2012). Despite this seemingly negligible amount of latent HIV present under ART, signs of the infection persist, including immune activation, low CD4 counts and increased risk for a number of co-morbidities (Deeks et al., 2013). Moreover, HIV replication resumes quickly when ART is discontinued, although a cellular and humoral immune response is present (Davey, Jr. et al., 1999).

Evidence is accumulating that extracellular vesicles not only play a role in cancer (Greening et al., 2015) but also in viral infections (Meckes, Jr., 2015). The membrane-enclosed viral-like structures are found at high levels in plasma, contain numerous effectors including enzymes, proteins, and RNAs (Raposo and Stoorvogel, 2013; Konadu et al., 2015) and are secreted continuously by cells with activated endo- and exocytosis (Baur, 2011). The latter may in part explain why tumor- as well as HIV-infected cells shed high numbers of EV (Skog et al., 2008; Muratori et al., 2009). In viral infections they seem to facilitate the spread of the virus, a finding that has also been suggested for HIV (Feng et al., 2013; Arenaccio et al., 2014; Meckes, Jr., 2015).

Our previous work suggested that large amounts of extracellular vesicles (EV) are secreted by HIV-infected cells (Lee et al., 2013; Muratori et al., 2009), which was confirmed by additional work (Lenassi et al., 2010; Narayanan et al., 2013; Shelton et al., 2012). Vesicle secretion was induced by the viral pathogenesis factor Nef and linked to Nef-mediated activation of ADAM17

at the plasma membrane. From there, both factors were shuttled into EV in a Paxillin-dependent mechanism. These in vitro vesicles were able to induce the release of TNF when ingested by resting PBMC. So far it was not clear whether these mechanisms occurred in vivo, what effect(s) they would induce and whether they were linked to HIV-associated immune pathogenesis. Here we demonstrate that HIV pEV contain a number of pro-inflammatory factors as well as the viral accessory proteins Nef and Vpu, are persistently upregulated despite ART and correlate significantly with pathogenesis in chronic infection. Importantly our results point to a so far not recognized cell compartment with ongoing viral activity under ART.

Materials and Methods

Nef antibodies and detection reagents

Different anti-Nef antibodies and reagents were used: (1) anti-Nef JR6, a mouse monoclonal antibody (Abcam ab42358); (2) anti-Nef 2A3, a mouse monoclonal antibody (Abcam ab77172); (3 and 4) anti-Nef sheep serum, either as a purified biotinylated polyclonal antibody or non-labeled (both from NEXT Biomed, Helsinki); (5) anti-Nef polyclonal serum (provided by Mark Harris, Leed University). All Nef-antibodies were used to demonstrate the presence of Nef in pEV. For immunoblotting JR6 turned out to have the highest sensitivity and specificity as judged by the ratio of Nef vs. background staining. For immunohistochemistry we used the biotinylated Nef sheep serum and the JR6 antibody. To confirm Nef in pEV, we also employed the recombinant Neffin construct, comprised of a 118 aa llama Ig heavy chain variable domain fragment (VHH) fused to a ligand-tailored 57 aa SH3 domain (Jarviluoma et al., 2012) and immunoprecipitated Nef from plasma (data not shown).

Antibodies

The following antibodies were used for immunostaining, flow cytometry or immunoblotting:
anti-ADAM10 (mouse monoclonal, Abcam ab73402), anti-ADAM10-PE (mouse monoclonal anti-ADAM17 (rabbit polyclonal, Cell Signaling 3976), anti-alpha-smooth muscle actin-FITC (Sigma-Aldrich, F3777), anti-TNF (rabbit monoclonal, Cell Signaling 6945), anti-Gag p24 (mouse monoclonal, Abcam ab9071), anti-CD81 (mouse monoclonal, BD Biosciences 555675), anti-Paxillin (mouse monoclonal, Millipore 05-417), anti-Tsg101 (mouse monoclonal, Santa Cruz Biotecnology sc-7964), anti-HLAI (mouse monoclonal, BD Biosciences 555551), anti-HLAII (mouse monoclonal, Abcam ab20181), anti-Vpu (rabbit polyclonal, Biozol FBX-VPU-101AP-100), anti-CD1c-PE (mouse monoclonal, Miltenyi Biotec, 130-90-007), anti-CD14-FITC (mouse monoclonal, Miltenyi Biotec, 130-080-701), anti-CD19-APC (mouse monoclonal, Miltenyi Biotec, 130-091-247), anti-Integrin $\alpha v\beta 3$ (mouse monoclonal, Abcam ab78289), Propidium iodide (Genaxxon bioscience, M3181.0010), DAPI (4',6-diamidino-2-phenylindole, Biomol ABD-17510). Primary antibodies were used at 1–2 µg ml^{-1} for immunoblotting, 2 µg ml^{-1} for immunofluorescence and 5–10 µg ml^{-1} for FACS analysis. The following secondary antibodies

were used: Alexa Fluor 488 goat anti-mouse and Alexa Fluor 555 goat anti-rabbit IgG (both from Life Technologies) and anti-mouse IgG-HRP conjugate and anti-rabbit IgG-HRP conjugate (both from Cell Signaling).

DNA constructs and transfection

Expression plasmids for Nef and Nef-cofactors (hnRNPK, PKCδ, Lck) were described previously (Lee et al., 2013). The HIV-Δenv (pNL-4.3Δenv (Clavel et al., 1989)) expression plasmid was kindly provided by U. Schubert (Department of Virology, University of Erlangen). For immunoblotting experiments, plasmids were transfected with Lipofectamine® LTX with Plus™ Reagent (Invitrogen) according to the manufacturer's instructions, or using the classical calcium phosphate procedure. Cells were used for experiments 24-72 h after transfection.

ADAM17/α-secretase acitivity assay

The assay was performed essentially as described previously (Lee et al., 2013) using a commercial, SensoLyte®520 α-Secretase Activity Assay Kit (AnaSpec 72085), according to the manufacturer's instructions. Briefly, we placed sucrose gradient purified pEV (the equivalent of 1 ml plasma) on a 96-well, black, flat bottom plate (Greiner 655900) and added a 5-FAM (fluorophore) and QXL™ 520 (quencher) labeled FRET peptide substrate for continuous measurement of enzyme activity. Upon cleavage of the FRET peptide by the active enzyme, the fluorescence of 5-FAM is recovered and continuously monitored at excitation/emission = 490 nm/520 nm by a preheated (37 °C) TECAN infinite M200 Pro plate reader.

Patient material

Patient material was obtained from patients of the HIV-clinic (headed by T. Harrer) at the Department of Medicine 3, University Hospital Erlangen. Plasma was drawn from patients after informed consent and approval of the local ethics committee. All procedures were pursued in accordance with the Declaration of Helsinki, with the patient's Guardian Informed Consent and the approval from the Institutional Review Board. At the time of sampling, non-viremic HIV patients were under ART for prolonged periods without detectable viral load (<20 viral copies/ml), while viremic patients (for viral copy number see Supplement Table S1) were untreated or had just started treatment. CD4 and CD8 counts (cells/μl blood) were determined by the Department of Medicine 3 and viral copies number (copies/ml blood) by the Department of Virology in Erlangen. In general, 6-7 ml of plasma was obtained from each individual per visit.

Immunostaining, Confocal microscopy and FACS analysis

For detection of Nef by immunofluorescence, monocytes were separated from the non-adherent fraction (NAF) by plastic adherence on cell culture flasks and cultured in RPMI (Sigma-Aldrich) including supplements. In HIV pEV incubation experiments, 3.0 x 10^5 monocytes were

seeded in a 12 well plate and 10 µg of sucrose gradient purified HIV pEV were added and incubated overnight at 37 °C under 5% CO_2. Then monocytes were harvested and 1.0 - 2.5 x 10^5 cells were seeded on a Poly-(L)-Lysine (Sigma Aldrich) coated cover slips. The cells adhered for 2 h at 37 °C under 5% CO_2 and were fixed thereafter (3% PFA for 30 min at room temperature followed with three washes with PBS/1% BSA). Then cells were permeabilized (0.1% Triton X-100/1% BSA) and immunostained by standard procedures (primary and secondary antibodies). Finally, the cells were washed 30 min with PBS/1% BSA and mounted with Entellan (Merck 1079610100). Fixed samples were imaged with a laser scanning confocal microscope (LSM-780; Zeiss) equipped with a 63x objective. For Alexa488 the illumination was set at 488 nm and emissions were collected between 506 and 583 nm. For Alexa555 the illumination was at 561 nm and emission collected between 574 and 667 nm. Detecting DAPI, illumination was set to 405 nm and emission collected between 410 and 495 nm.

For FACS analysis, $CD1c^+$ cells from at least 1.0 x 10^7 PBMC were isolated following the protocol of the $CD1c^+$ ($BDCA\text{-}1^+$) Dendritic Cell Isolation Kit (Miltenyi Biotec 130-090-506), but without depletion of CD19 cells. Cells were stained with fluorochrome-conjugated antibodies and flow cytometric analysis was done using a FACS Canto II flow cytometer (BD Bioscience). Data were analyzed with the FCS Express 4 (De Novo Software) software. $CD1c^+$ $CD14^+$ cells were analyzed in the $CD19^-$ gated fraction of cells, as CD1c is also expressed on a subset of B cells. CD19 MACS beads (Miltenyi Biotec 130-050-301) and CD14 Magnetic particles (BD Bioscience 557769) were used for positive selection following the magnetic separation protocol of the manufacturer.

Micro-RNA microarray

The pEV were purified from equal volumes of pooled or non-pooled platelet poor plasma supplemented with BHRF1-2* miRNA as spike-in control (see below) and pelleted. The pEV pellets were then dissolved in 700 µl of Qiazol and total RNA was isolated using Qiagen miRNeasy Mini Kits (Qiagen 217004). The extracted RNA was sent on dry ice to Miltenyi Biotec. 100 ng total RNA was concentrated to 50 ng/µL and Cy3-labelled using Agilent's miRNA Complete Labeling and Hyb Kit (Agilent Technologies, 5190-0456). After purification through Micro Bio Spin Columns (Bio Rad, 732-6221) the total RNA samples were hybridized for 20 hours at 55°C to human miRNA microarrays (Agilent, Version V16, 8x60K). The microarrays were washed in Triton-containing washing buffer as recommended by the manufacturer and scanned with the Agilent's Microarray Scanner System (Agilent Technologies). The image files were analyzed and processed by Agilent Feature Extraction Software (Version 10.7.3.1). The received miRNA expression data was analyzed for logarithmic dot plots using Excel 2010 (Microsoft) and for cluster analysis MultiExperiment Viewer Version 4.9 (MeV, http://www.tm4.org/mev.html). Logarithmic dot plots and average miRNA fold change assessments were generated analyzing gradient purified pEV from pooled HIV and healthy plasma. Micro-RNA cluster analysis (Figure 1B) was performed for individual plasma samples

(14 ml) from 2 viremic, 2 non-viremic HIV patients and 8 healthy individuals based on Euclidean distance. For pairwise comparison of patient groups (Figure 1a, Fig. S1a) means of each detected miRNA were calculated within each group and plotted on a logarithmic scale.

EV depletion of FCS and human serum for cell culture

To assure EV generated from cell culture were not contaminated by outside sources, heat inactivated FCS and human serum for medium supplementation were depleted of vesicles by ultracentrifugation for 18 h at 110,000 g, 4 °C before use.

Isolation and purification of EV

EV purification was performed essentially as described previously (Muratori et al., 2009; Thery et al., 2009). Briefly, supernatants were collected after 48 h and centrifuged for 20 min at 2,000 g, 30 min at 10,000 g and ultra-centrifuged for 1 h at 100,000 g. Pellets were resuspended in 35 ml PBS and centrifuged at 100,000 g for 1 h. Pellets were resuspended in 100 µl PBS and considered as EV preparations.

For EV purification from patient samples, 30 ml blood plasma was diluted with 30 ml PBS and centrifuged for 30 min at 2,000 g, 45 min at 12,000 g and ultra-centrifuged for 2 h at 110,000 g. Pellets were resuspended in 30 ml PBS and centrifuged at 110,000 g for 1 h. Pellets were again resuspended in 100 µl PBS and considered as EV preparations. For further purification, EV were diluted in 2 ml of 2.5 M sucrose, 20 mM Hepes/NaOH, pH 7.4 and a linear sucrose gradient (2 - 0,25 M sucrose, 20 mM Hepes/NaOH pH 7.4) was layered on top of the EV suspension. The samples were then centrifuged at 210,000 g for 15 h. Gradient fractions were collected and the refractive index was determined. Each fraction was diluted in 10 ml PBS and ultra-centrifuged for 1 h at 110,000 g. Pellets were solubilized in SDS sample buffer or resuspended in 100 µl PBS and analyzed by immunoblotting or Cytokine/Chemokine/ soluble Factor (CCF) protein array (see supplementary information).

To validate our centrifugation-based pEV isolation protocol, we generated an EV spike-in control (from a stable cell line producing EV), containing an EBV-derived miRNA (BHRF1-2*) that was not found in human pEV-miRNAs, but was detectable by the miRNA microarray (Agilent). After spike-in, BHRF1-2* miRNA was readily detected with comparable efficiency in 4 different plasma samples (data not shown).

Immunoisolation of pEV/EV by magnetic beads

Antibodies were coupled to magnetic microbeads by a Miltenyi Biotec (Bergisch Gladbach, Germany). For isolation of pEV, 2 ml blood plasma was diluted with 2 ml PBS and 50 µl of antibody-coupled beads were added for 1h and subsequently subjected to magnetic immunoisolation with MACS® Technology (Miltenyi Biotec) using MS columns. To purify EV from cells, cell cultured supernatants were collected and were purified by combining

differential centrifugation and column-based bead isolation. The vesicles were finally eluted with 45µl of hot (95°C) SDS sample buffer and all of the vesicle lysate was subsequently analyzed by western blot. The column flow-through was collected and centrifuged at 110,000 g (pEV) or 100,000 g (EV from cells) for 1 h. Pellets were solubilized in SDS sample buffer and analyzed by western blot.

Screening of primary hybridoma supernatants directed against Nef EV

Latex beads were coated with 10 µl Nef EV generated from Nef transfected 293T cells as described previously (Lee et al., 2013). Subsequently the beads were incubated with 10 µl primary hybridoma supernatant (host: mouse) dissolved in 50 µl PBS/0.5% BSA for 30 minutes at 4°C. 200 µl PBS/0.5% BSA was added and the sample was centrifuged at 1500 g for 3 min at RT. The pellet was resuspended in 200 µl PBS/0.5% BSA and incubated with 1 µl anti-mouse Alexa Fluor® 488 labeled secondary antibody for 30 min at 4°C and subsequently washed twice before a FACS measurement was carried out. Primary screening was done with 262 monoclonal antibodies generated against EV antigens. The candidates of EV specific antigens were selected and analyzed by FACS to identify antibodies specifically binding to Nef EV.

Peripheral blood mononuclear cell (PBMC) preparation

Leukoreduction system chambers (LRSCs) from healthy donors were acquired after plateletpheresis. The resulting platelet free cell sample was diluted 1:2 in PBS and the PBMC containing buffy coat was isolated after density gradient centrifugation on Lymphoprep (Axix Shield 1114544) at 500 g for 30 min at room temperature. PBMCs were then washed 3 times in PBS/1 mM EDTA; 1. wash: 282 g, 15 min, 4 °C; 2. wash: 190 g, 10 min, 4 °C; 3. wash: 115 g, 12 min, 4 °C).

Particle quantification

Sucrose purified pEV were diluted 1:1,000,000 for HIV patients and 1:1,000 for healthy donors in PBS. The pEVs numbers were quantified via particle tracking analysis on a commercially available ZetaView particle tracker from ParticleMetrix (Germany) using a 10 µl aliquot of the diluted samples. The concentration of pEV was then calculated using the appropriate dilution factors.

Measurement of Cytokine Secretion

PBMCs or positive-selected cells (1 x 10^5) were added to each well of a 96-well-U-bottom plate (BD Biosciences) in a total volume of 200 µl medium. Cytokines in the supernatant (200 µl) were measured via the CBA (Cytometric Bead Array) Human Th1/Th2/Th17 kit (BD Biosciences 560484) or Human Soluble Protein Flex Set System (BD Biosciences 558265).

Image quantifications of immunoblotting

All image quantifications were performed with ImageJ software (NIH). The quantified data were analyzed using Excel 2010 (Microsoft) for statistical analysis.

Human cytokine/chemokine/soluble factor (CCF) array

Purified EV from sucrose gradient fractions were applied to the RayBio Human Cytokine Array C-S (Hölzel Diagnostika, AAH-CYT-1000-2) according to the manufacturer's instructions. Cytokines were analyzed and identified based on a table presented in supplement material.

Results

High levels of pEV in viremic and non-viremic HIV infection

To quantify pEV in blood of infected individuals, we measured pEV-derived miRNAs (Valadi et al., 2007; Aqil et al., 2014). After pEV were purified by sucrose gradient from a pool of 4 viremic or non-viremic patients (patient details per experiment in Table S1), extracted miRNAs were assessed by miRNA microarray. Levels of detected miRNAs were on average 25.9-fold higher than in healthy controls (Fig. 1a, left panel), but surprisingly slightly lower than levels measured in non-viremic patients (right panel). Plasma samples from single individuals w/wo viremia and 8 controls were analyzed accordingly and gave similar results (Fig. 1b and Fig. S1a).

Measuring the total protein content in pEV gradient fractions (as in Fig. 1d, upper panels), we found an increase of about 18 to 22-fold over healthy controls in both HIV groups (Fig. 1c). The slightly higher protein levels in viremic patients might have been attributed to the presence of viral particles (see p24 in Fig. 2a). Similarly, a particle number and size analysis revealed a 12 - 28-fold increase (median: 17.9) of pEV over healthy controls as well as a broader size range of the particles (Fig. 1d and e). Together these results suggested a sustained increase of HIV pEV despite ART.

HIV pEV contain viral accessory proteins and inflammatory effectors

Similar as observed previously, purified HIV pEV contained Nef and activated ADAM17 and -10 proteases as well as classical EV-markers (CD63, CD81) (Lee et al., 2013; Khan et al., 2015). In addition, we detected TNF and its precursor (Fig. 2a). ADAM17 activation was only seen in fractions where Nef was present, evidenced by the cleavage of the TNF precursor into its mature form (red boxes and arrows). To our great surprise, this pEV protein profile was identical in viremic and non-viremic patients. Blotting for p24 Gag confirmed the presence of viral particles in viremic patients. In addition, p24 floated slightly different than pEV, pointing to a slight size/density difference of viral particles (Fig. 2a). However, we cannot exclude that p24 was also present in pEV. Nevertheless the presence of p24 was an indication for viral replication. Non-viremic HIV pEV also contained Vpu, as shown with different plasma samples (Fig. S1b; Fig. 3b and 4a, b). Supporting this finding, the uploading of Vpu into EV was confirmed

by transient transfection experiments (Fig. S1c). These results suggested continuous expression of viral accessory proteins in the absence of productive replication. As Nef induces the secretion of EV, this seemingly explained the unabated high levels of pEV despite ART.

Searching for potential differences between viremic and non-viremic-derived pEV, we analyzed whether they harbored additional cytokines, chemokines and soluble factors (hereafter referred to as CCF). Purified pEV from a plasma pool of clinically healthy non-viremic patients (CD4>800/μl) and viremic patients with low CD4 counts (<250/μl), as well as healthy volunteers (details in Tables S1 and S2) were analyzed for 120 CCF by protein array (list of all CCF in Supplement Methods). Whereas healthy pEV contained 3 CCF, HIV pEV harbored as many as 23 in readily detectable amounts (Fig. 2b). Both HIV groups showed significant differences (red boxes). In general, viremic patients with low CD4 counts harbored more and higher levels of CCF including a number of pro-inflammatory effectors (e.g. TNF, IL-12p40, sIL-6R, sTNF-RI, GRO). Overall, however, both profiles had a similar pattern. This pattern suggested that the vesicles originated from a myeloid/macrophage-like cell population (e.g. IL-12p40, GRO, NAP-2).

HIV pEV constitute a pEV subclass induced by αvβ3 activation

Since pEV constitute a mix of different vesicles from different cell populations, we asked whether HIV accessory proteins and the pro-inflammatory effectors were uploaded into the same pEV. We screened a panel of 262 monoclonal antibodies generated against EV antigens. The selected EV specific candidates were analyzed to identify antibodies specifically binding to Nef-induced and Nef-containing EV. We identified one antibody (2H4) that, when coupled to magnetic beads (Fig. S2a), captured seemingly 100% of Nef-containing pEV (Fig. 3a, compare red boxes). Along with Nef, all activated ADAM17 and 10, mature TNF and also Vpu were found. Surprisingly, many common vesicle markers (Tsg101, CD81, CD25, DC-SIGN) were not detected (Fig. 3a, green boxes), while CD63 and HLA-I were present. When the CCF profile was analyzed following 2H4-bead isolation, most effectors, including those with a pro-inflammatory effect and putative myeloid origin, co-precipitated with the bead fraction in an all or nothing fashion (Fig. 3b). This and the distinct surface marker profile implicated that Nef pEV constituted a specific subclass of vesicles, potentially distinct from multivesicular body (MVB)-derived classical exosomes. The latter are typically secreted in an ESCRT (Tsg101)-dependent pathway (Colombo et al., 2013), which we did not detect in Nef-containing pEV. Together these results confirmed that HIV accessory proteins were co-packaged into pEV with an array of pro-inflammatory effectors and chemokines.

Using MALDI TOF we identified αvβ3 as the binding antigen of 2H4 (Fig. S2b). Control pEV from healthy individuals harbored αvβ3, but were not recognized/isolated by 2H4-coupled beads as revealed by blotting with a commercial αvβ3 antibody (Fig. 3c, red boxes). Conversely, 2H4 captured pEV when Nef, active ADAM17 and mature TNF were present (Fig. 3a and c, see TNF). Together this suggested that 2H4 bound an activation-induced epitope of αvβ3 and implicated

that the integrin was activated when HIV pEV were induced by Nef. Again, the absence of Tsg101 and CD81 in the bead fraction suggested that Nef/αvβ3 pEV constituted a subclass of vesicles distinct from MVB-derived exosomes (Fig. 3c). Supporting the assumption that Nef activated αvβ3, a co-transfection of Nef with cofactors hnRNPK, Lck and PKCδ, which induces Paxillin phosphorylation in 293T cells (Lee et al., 2013), also stimulated the phosphorylation of Pyk2 and PLCγ (Fig. 3e). In their activated forms these factors form a complex with αvβ3 (Pfaff and Jurdic, 2001; Nakamura et al., 2001). These results indicated that αvβ3 activation was required for the induction of HIV pEV.

Peripheral mononuclear cells ingest HIV pEV and secrete inflammatory cytokines

Inflammatory peripheral mononuclear cells are a hallmark of chronic HIV infection and correlate with the development ART-resistant pathogenesis (Wilson et al., 2014; Sandler et al., 2011). Since mononuclear cells efficiently incorporate EV (Lee et al., 2013), we asked whether HIV pEV were involved in this patho-mechanism. To demonstrate a possible uptake of HIV vesicles, plastic adherent mononuclear cells from different non-viremic individuals were stained for Nef, Vpu and p24 Gag. Indeed, an astonishing 47 - 72% of these cells contained Nef, whereas Vpu and p24 were detected at much lower frequency, 3 - 12% and 1 - 3% respectively (Fig. 4a and c). We explained this unexpected high frequency of Nef-positive cells with the high concentration and efficient uptake of HIV pEV. To confirm this assumption, HIV non-viremic pEV were incubated with mononuclear cells from healthy donors and stained as above. Positive staining for Nef and Vpu indeed suggested a vesicle-mediated transfer of these proteins (Fig. 4b), and confirmed the presence of Nef/Vpu-containing pEV in non-viremic patients. Notably, p24-positive cells were not detected, confirming that p24 was not present in HIV pEV. To further support these surprising findings, primary mononuclear cells were analyzed for Nef and ADAM17 by Western blot. In line with the last results, only the HIV mononuclear cells harbored activated ADAM17 and Nef (red box) (Fig. 4d).

Under inflammatory conditions, monocyte-derived $CD1c^+$ $CD14^+$ dendritic cells develop (Segura et al., 2013). We found that $CD1c^+$ $CD14^+$ $CD19^-$ cells increased in PBMC of non-viremic patients by about 10-fold over controls, to approximately 0.2% +/- 0.17% of PBMC (Fig. 5a and b). All $CD1c^+$ cells were Nef-positive and developed CD14 granules as if generated for secretion (Fig. 5a). Resting PBMC of non-viremic individuals secreted significant amounts of TNF, IL-6 and IFNγ within 12 hours, an effect that was abolished when the $CD1c^+$ cells were depleted (Fig. 5c). Positively selected $CD14^+$ cells also secreted TNF and IL-6, whilst $CD1c^+$- or $CD1c^+$ $CD14^+$ $CD19^-$-selected cells were not viable in culture in our hands (Fig. 5d and data not shown). For control, $CD1c^+$ $CD19^+$ cells (B-cells) were selected and cultured, but secreted no cytokines (Fig. 5d). Collectively these data suggested that HIV pEV were involved in the induction of inflammatory mononuclear cells.

pEV-derived Nef and ADAM17 activity correlate with low T cell counts

Since pEV are highly concentrated and also ingested by T cells (Lee et al., 2013; Gutierrez-Vazquez et al., 2013), we asked whether inflammatory pEV modulated the T cell count in HIV infection. Multiple pEV-derived factors and plasma p24 Gag levels from 17 non-viremic and 16 viremic patients were analyzed by Western blot and quantified by ImageJ software (Schneider et al., 2012). Results were correlated with CD4 and CD8 counts and viral copy numbers. Validating our approach, viral copy numbers vs. p24 levels as well as Nef vs. ADAM17 correlated visibly by Western blot (Fig 6a, arrows) and gave the expected significant positive Pearson correlation coefficient (Fig. 6b, upper panels).

In both patient groups the Western blots revealed an inverse relationship between the presence of either Nef or active ADAM17 and CD4 counts. Supporting this finding, there was also a visible inverse correlation with Paxillin, which is required for ADAM17 uploading into pEV (Lee et al., 2013). Conversely, ADAM10, Tsg101, HLA-I, and HLA-DR were evenly present (Fig. 6A left panel, arrows, and Fig. S3a and S4b). The calculated correlations between Nef, or ADAM17, and CD4 counts were highly significant (Fig. 6b, red boxes, and Fig. S5a). Similar but less stringent correlations were seen with respect to CD8 counts, particularly in viremic patients (Fig. 6b, yellow boxes and S5b). Neither viral copy number nor p24 correlated with CD4, CD8, Nef or ADAM17 respectively, as observed in Western blots (Fig. 6a, right panel, arrows and Fig. S4a) or determined by calculation (Fig. 6b, grey boxes). Also, p24 levels did not correlate with pEV Nef levels, suggesting that they derived from different sources (Fig. 6a right panels). Although the number of analyzed patients was low, the stringent results and internal validations implied that the ADAM17-containig HIV pEV correlated with T cell levels in viremic and non-viremic infection.

To support this conclusion, pEV from viremic and non-viremic patients with different CD4 counts were analyzed for ADAM17 protease activity using a pro-TNF sequence-based FRET peptide cleavage assay (AnaSpec). The results confirmed an inverse relationship between ADAM17 activity and individual CD4 levels irrespectively of the presence of viral particles (Fig. 6c, left panel). Notably, the three healthy controls revealed no ADAM17 activity at all. To solidify this finding, we assayed three plasma pools derived from non-viremic patients only, representing different ranges of CD4 levels. The result confirmed the inverse relationship between CD4 count and ADAM17 activity (Fig. 6c right panel). Together with the Western blot analysis these findings suggested a link between Nef-mediated ADAM17 activation and lower CD4 counts.

HIV pEV are secreted in part by PBMC

The CCF profile of HIV pEV pointed at a myeloid compartment as their cellular source; however this profile did not exclude T cells. Non-stimulated primary T cells from infected or healthy individuals produced only negligible amounts of EV in vitro, insufficient to give a CCF signal

(data not shown). Conversely, Jurkat T cells transfected with an HIV-Δenv viral construct (expression control in Fig. S6) did secrete EV with some lymphocyte-typical CCF, including TNF. However, most of these factors were not detected in HIV pEV (Fig. 7). Thus we analyzed EV shed by non-stimulated PBMC from 7 non-viremic patients in 48h (pooled supernatants). The results revealed a CCF pattern that showed some overlap with HIV pEV (7 of 23 CCF; Fig. 7, red boxes). In addition some T cell typical factors were detected (blue boxes), implying that the interaction of different PBMC fractions stimulated EV secretion also from T cells. Therefore it seemed possible that at least a fraction of HIV pEV derived from PBMC. However, since PBMC from non-viremic individuals are not productively infected by HIV, it appeared unlikely that the bulk of HIV pEV were produced by PBMC and thus must have originated from a different myeloid cell pool.

Discussion

By analyzing primary material from a total of 166 HIV patients we suggest that HIV Nef acts at least in part by the induction of pro-inflammatory pEV. We have previously suggested a model of how Nef/ADAM17-containing EV induce the secretion of TNF in host and target cells (Lee et al., 2013). It is tempting to speculate that this mechanism renders resting T cells permissive for the viral infection as suggested recently (Arenaccio et al., 2014). Here we asked whether HIV pEV have detrimental effects on the immune system and found a surprisingly strong correlation with immune pathogenesis, seemingly due to the pro-inflammatory nature of these vesicles.

Plasma EV of infected individuals were loaded with pro-inflammatory effectors, while healthy controls harbored none. This striking difference could be a consequence of Nef-mediated activation of ADAM proteases. However, it is also possible that the viral protein triggered a host inflammatory reaction. Many ADAM proteases associate with Integrins at the plasma membrane (Murphy, 2008) and activated Integrins induce the formation of vesicles (Caswell et al., 2009). Thus a putative host inflammatory pEV response could be induced by Integrin activation. Potentially this is mimicked by Nef through targeting of $\alpha v\beta 3$, similar as we have suggested before (Witte et al., 2004).

The high percentage of Nef-positive mononuclear cells indirectly confirmed our observation that Nef pEV levels are significantly increased in non-viremic patients. It is conceivable to assume that monocytes ingesting large amounts of pro-inflammatory pEV undergo functional changes and acquire an inflammatory phenotype that is typically seen in chronic HIV infection. We documented such a cellular differentiation by describing a Nef^+ $CD1c^+$ $CD14^+$ $CD19^-$ cell type that could be considered an inflammatory immature dendritic cell. Notably, this cell population showed a strong production of inflammatory cytokines in vitro. This does not exclude that other pEV acquiring monocytes were non-productive, as we measured only some cytokines at an early time point (12h). Therefore, most Nef-containing mononuclear cells could have a role in the development of secondary inflammatory effects in blood and tissue.

Although the low number of patients analyzed precludes final conclusions, the stringent correlations between T cell levels, Nef levels and ADAM17-activity corroborated that Nef activates this protease and hints at a particular role of ADAM17 in T cell decline. The mechanism is not obvious but may involve the TNF/TNF-receptor-I/II-mediated regulation of apoptosis/anti-apoptosis in T cells. These proteins are substrates of ADAM17 and increased levels of their soluble forms correlate with disease progression (Zangerle et al., 1994). The latter is an independent confirmation for the correlation between active ADAM17 and HIV pathogenesis.

Surprisingly, pEV levels did not decline during ART, suggesting that they did not derive from a T cell compartment as the latter sees dramatic recovery upon treatment. Supporting this conclusion we saw no correlation between Gag p24 and pEV-derived Nef levels in viremic patients and HIV-transfected Jurkat cells did not produce a CCF pattern similar to that of HIV pEV. We therefore have to predict the existence of an infected myeloid or myeloid-like compartment, which may produce predominantly spliced Nef and Vpu mRNA message despite effective treatment. In line with our findings, the presence of SIV viral sanctuaries could be demonstrated in numerous cellular compartments despite efficient ART (North et al., 2010). The pEV-producing cells could be, for example, stem cell-like precursor cells in different organs that are long-lived and promote HIV immune pathogenesis independently of viral replication. It will be interesting to identify these cells.

In summary our findings suggest that high levels of inflammatory pEV have an important role in the pathogenesis of viremic as well as chronic (i.e. non-viremic) HIV infection. This finding also point to a hidden but highly active HIV compartment that is not suppressed by ART. Therefore monitoring pEV Nef levels or ADAM17 activity could have diagnostic value in clinical management of HIV infection. In addition, our findings may point out new opportunities for treatment interventions aiming to reduce immune activation in chronic HIV disease.

Conflict of Interest:

Nina Koliha and Stefan Wild are employees of Miltenyi Biotec GmbH.

Contributions: The project was conceptualized and coordinated by A.S.B. Substantial contributions to the work were made by J-H.L. (pEV purification, transfections, Western blots, protein array and antibody screening for Nef EV); S.Sch. and G.S. (PBMC analysis by FACS and cytokine secretion); W.X. (MALDI-TOF); J.D. (miRNA extraction and analysis); K.B. (Nef immunohistochemistry); N.K. and St.W. (miRNA assessment by micro array); S.W. (confocal imaging); T.H. (plasma and tissue sample analysis); O.F. and K.S. (expertise, feedback and reagents).

Acknowledgments: This work was supported by funds from the German Science Foundation (DFG): SFB 643 (J-H.L.) and BA961/3-1 (S.W.). J.D. was supported by funds from the German Federal Ministry of Education and Research (BMBF) under grant 01GU1107A. S. Sch. is supported by the IZKF Erlangen (Interdisziplinäre Zentrum für Klinische Forschung). C.O. is supported by the Comprehensive Cancer Center (CCC) Erlangen. K.B. is supported by funds from the European Union (HIVERA IRIFCURE). T.H. was supported by the Emerging Fields Program of the Friedrich-Alexander-University of Erlangen-Nürnberg. O.T.F acknowledges funding from the Deutsche Forschungsgemeinschaft (SFB1129 project 8) and the European union (IRIFCURE consortium). We would like to thank F. Dreyer for primary antibody screening for EV specific antigens, Hans-Martin Jäck, Jürgen Wittmann, Iryna Prots for helping to establish the stable cell line producing the spike-in control for the pEV miRNA purification, and Miguel Lamas-Murua for helping to make a basis of Vpu detection in pEV.

References

Reference List

Aqil,M., Naqvi,A.R., Mallik,S., Bandyopadhyay,S., Maulik,U., and Jameel,S. (2014). The HIV Nef protein modulates cellular and exosomal miRNA profiles in human monocytic cells. J. Extracell. Vesicles. *3*.

Arenaccio,C., Chiozzini,C., Columba-Cabezas,S., Manfredi,F., Affabris,E., Baur,A., and Federico,M. (2014). Exosomes from human immunodeficiency virus type 1 (HIV-1)-infected cells license quiescent CD4+ T lymphocytes to replicate HIV-1 through a Nef- and ADAM17-dependent mechanism. J. Virol. *88*, 11529-11539.

Baur,A.S. (2011). HIV-Nef and AIDS pathogenesis: are we barking up the wrong tree? Trends Microbiol. *19*, 435-440.

Caswell,P.T., Vadrevu,S., and Norman,J.C. (2009). Integrins: masters and slaves of endocytic transport. Nat. Rev. Mol. Cell Biol. *10*, 843-853.

Clavel,F., Hoggan,M.D., Willey,R.L., Strebel,K., Martin,M.A., and Repaske,R. (1989). Genetic recombination of human immunodeficiency virus. J. Virol. *63*, 1455-1459.

Davey,R.T., Jr., Bhat,N., Yoder,C., Chun,T.W., Metcalf,J.A., Dewar,R., Natarajan,V., Lempicki,R.A., Adelsberger,J.W., Miller,K.D., Kovacs,J.A., Polis,M.A., Walker,R.E., Falloon,J., Masur,H., Gee,D., Baseler,M., Dimitrov,D.S., Fauci,A.S., and Lane,H.C. (1999). HIV-1 and T cell dynamics after interruption of highly active antiretroviral therapy (HAART) in patients with a history of sustained viral suppression. Proc. Natl. Acad. Sci. U. S. A *96*, 15109-15114.

Deeks,S.G., Lewin,S.R., and Havlir,D.V. (2013). The end of AIDS: HIV infection as a chronic disease. Lancet *382*, 1525-1533.

Doitsh,G., Galloway,N.L., Geng,X., Yang,Z., Monroe,K.M., Zepeda,O., Hunt,P.W., Hatano,H., Sowinski,S., Munoz-Arias,I., and Greene,W.C. (2014). Cell death by pyroptosis drives CD4 T-cell depletion in HIV-1 infection. Nature *505*, 509-514.

Eisele,E. and Siliciano,R.F. (2012). Redefining the viral reservoirs that prevent HIV-1 eradication. Immunity. *37*, 377-388.

Eriksson,S., Graf,E.H., Dahl,V., Strain,M.C., Yukl,S.A., Lysenko,E.S., Bosch,R.J., Lai,J., Chioma,S., Emad,F., Abdel-Mohsen,M., Hoh,R., Hecht,F., Hunt,P., Somsouk,M., Wong,J., Johnston,R., Siliciano,R.F., Richman,D.D., O'Doherty,U., Palmer,S., Deeks,S.G., and Siliciano,J.D. (2013). Comparative analysis of measures of viral reservoirs in HIV-1 eradication studies. PLoS. Pathog. *9*, e1003174.

Feng,Z., Hensley,L., McKnight,K.L., Hu,F., Madden,V., Ping,L., Jeong,S.H., Walker,C., Lanford,R.E., and Lemon,S.M. (2013). A pathogenic picornavirus acquires an envelope by hijacking cellular membranes. Nature *496*, 367-371.

Greening,D.W., Gopal,S.K., Xu,R., Simpson,R.J., and Chen,W. (2015). Exosomes and their roles in immune regulation and cancer. Semin. Cell Dev. Biol. *40*, 72-81.

Gutierrez-Vazquez,C., Villarroya-Beltri,C., Mittelbrunn,M., and Sanchez-Madrid,F. (2013). Transfer of extracellular vesicles during immune cell-cell interactions. Immunol. Rev. *251*, 125-142.

Ho,D.D., Neumann,A.U., Perelson,A.S., Chen,W., Leonard,J.M., and Markowitz,M. (1995). Rapid turnover of plasma virions and CD4 lymphocytes in HIV-1 infection. Nature *373*, 123-126.

Jarviluoma,A., Strandin,T., Lulf,S., Bouchet,J., Makela,A.R., Geyer,M., Benichou,S., and Saksela,K. (2012). High-affinity target binding engineered via fusion of a single-domain antibody fragment with a ligand-tailored SH3 domain. PLoS. One. *7*, e40331.

Khan,M.B., Lang,M.J., Huang,M.B., Raymond,A., Bond,V.C., Shiramizu,B., and Powell,M.D. (2015). Nef exosomes isolated from the plasma of individuals with HIV-associated dementia (HAD) can induce Abeta secretion in SH-SY5Y neural cells. J. Neurovirol.

Konadu,K.A., Chu,J., Huang,M.B., Amancha,P.K., Armstrong,W., Powell,M.D., Villinger,F., and Bond,V.C. (2015). Association of Cytokines With Exosomes in the Plasma of HIV-1-Seropositive Individuals. J. Infect. Dis. *211*, 1712-1716.

Lee,J.H., Wittki,S., Brau,T., Dreyer,F.S., Kratzel,K., Dindorf,J., Johnston,I.C., Gross,S., Kremmer,E., Zeidler,R., Schlotzer-Schrehardt,U., Lichtenheld,M., Saksela,K., Harrer,T., Schuler,G., Federico,M., and Baur,A.S. (2013). HIV Nef, paxillin, and Pak1/2 regulate activation and secretion of TACE/ADAM10 proteases. Mol. Cell *49*, 668-679.

Lenassi,M., Cagney,G., Liao,M., Vaupotic,T., Bartholomeeusen,K., Cheng,Y., Krogan,N.J., Plemenitas,A., and Peterlin,B.M. (2010). HIV Nef is secreted in exosomes and triggers apoptosis in bystander CD4+ T cells. Traffic. *11*, 110-122.

Meckes,D.G., Jr. (2015). Exosomal communication goes viral. J. Virol. *89*, 5200-5203.

Muratori,C., Cavallin,L.E., Kratzel,K., Tinari,A., De,M.A., Fais,S., D'Aloja,P., Federico,M., Vullo,V., Fomina,A., Mesri,E.A., Superti,F., and Baur,A.S. (2009). Massive secretion by T cells is caused by HIV Nef in infected cells and by Nef transfer to bystander cells. Cell Host. Microbe *6*, 218-230.

Murphy,G. (2008). The ADAMs: signalling scissors in the tumour microenvironment. Nat. Rev. Cancer *8*, 929-941.

Nakamura,I., Lipfert,L., Rodan,G.A., and Le,T.D. (2001). Convergence of alpha(v)beta(3) integrin- and macrophage colony stimulating factor-mediated signals on phospholipase Cgamma in prefusion osteoclasts. J. Cell Biol. *152*, 361-373.

Narayanan,A., Iordanskiy,S., Das,R., Van,D.R., Santos,S., Jaworski,E., Guendel,I., Sampey,G., Dalby,E., Iglesias-Ussel,M., Popratiloff,A., Hakami,R., Kehn-Hall,K., Young,M., Subra,C., Gilbert,C., Bailey,C., Romerio,F., and Kashanchi,F. (2013). Exosomes derived from HIV-1-infected cells contain trans-activation response element RNA. J. Biol. Chem. *288*, 20014-20033.

North,T.W., Higgins,J., Deere,J.D., Hayes,T.L., Villalobos,A., Adamson,L., Shacklett,B.L., Schinazi,R.F., and Luciw,P.A. (2010). Viral sanctuaries during highly active antiretroviral therapy in a nonhuman primate model for AIDS. J. Virol. *84*, 2913-2922.

Perelson,A.S., Neumann,A.U., Markowitz,M., Leonard,J.M., and Ho,D.D. (1996). HIV-1 dynamics in vivo: virion clearance rate, infected cell life-span, and viral generation time. Science *271*, 1582-1586.

Pfaff,M. and Jurdic,P. (2001). Podosomes in osteoclast-like cells: structural analysis and cooperative roles of paxillin, proline-rich tyrosine kinase 2 (Pyk2) and integrin alphaVbeta3. J. Cell Sci. *114*, 2775-2786.

Raposo,G. and Stoorvogel,W. (2013). Extracellular vesicles: exosomes, microvesicles, and friends. J. Cell Biol. *200*, 373-383.

Sandler,N.G., Wand,H., Roque,A., Law,M., Nason,M.C., Nixon,D.E., Pedersen,C., Ruxrungtham,K., Lewin,S.R., Emery,S., Neaton,J.D., Brenchley,J.M., Deeks,S.G., Sereti,I., and Douek,D.C. (2011). Plasma levels of soluble CD14 independently predict mortality in HIV infection. J. Infect. Dis. *203*, 780-790.

Schneider,C.A., Rasband,W.S., and Eliceiri,K.W. (2012). NIH Image to ImageJ: 25 years of image analysis. Nat. Methods *9*, 671-675.

Segura,E., Touzot,M., Bohineust,A., Cappuccio,A., Chiocchia,G., Hosmalin,A., Dalod,M., Soumelis,V., and Amigorena,S. (2013). Human inflammatory dendritic cells induce Th17 cell differentiation. Immunity. *38*, 336-348.

Shelton,M.N., Huang,M.B., Ali,S.A., Powell,M.D., and Bond,V.C. (2012). Secretion modification region-derived peptide disrupts HIV-1 Nef's interaction with mortalin and blocks virus and Nef exosome release. J. Virol. *86*, 406-419.

Skog,J., Wurdinger,T., van,R.S., Meijer,D.H., Gainche,L., Sena-Esteves,M., Curry,W.T., Jr., Carter,B.S., Krichevsky,A.M., and Breakefield,X.O. (2008). Glioblastoma microvesicles transport RNA and proteins that promote tumour growth and provide diagnostic biomarkers. Nat. Cell Biol. *10*, 1470-1476.

Thery,C., Ostrowski,M., and Segura,E. (2009). Membrane vesicles as conveyors of immune responses. Nat. Rev. Immunol. *9*, 581-593.

Valadi,H., Ekstrom,K., Bossios,A., Sjostrand,M., Lee,J.J., and Lotvall,J.O. (2007). Exosome-mediated transfer of mRNAs and microRNAs is a novel mechanism of genetic exchange between cells. Nat. Cell Biol. *9*, 654-659.

Wilson,E.M., Singh,A., Hullsiek,K.H., Gibson,D., Henry,W.K., Lichtenstein,K., Onen,N.F., Kojic,E., Patel,P., Brooks,J.T., Sereti,I., and Baker,J.V. (2014). Monocyte-Activation Phenotypes Are Associated With Biomarkers of Inflammation and Coagulation in Chronic HIV Infection. J. Infect. Dis. *210*, 1396-1406.

Witte,V., Laffert,B., Rosorius,O., Lischka,P., Blume,K., Galler,G., Stilper,A., Willbold,D., D'Aloja,P., Sixt,M., Kolanus,J., Ott,M., Kolanus,W., Schuler,G., and Baur,A.S. (2004). HIV-1 Nef mimics an integrin receptor signal that recruits the polycomb group protein Eed to the plasma membrane. Mol. Cell *13*, 179-190.

Zangerle,R., Gallati,H., Sarcletti,M., Weiss,G., Denz,H., Wachter,H., and Fuchs,D. (1994). Increased serum concentrations of soluble tumor necrosis factor receptors in HIV-infected individuals are associated with immune activation. J. Acquir. Immune. Defic. Syndr. *7*, 79-85.

Figure Legends

Figure 1: High levels of Nef-containing pEV in viremic and non-viremic HIV infection.

(**A**) Pairwise comparison of pEV miRNA levels obtained by miRNA micro arrays, derived from viremic HIV patients and healthy controls (left panel), and non-viremic patients (right panel). Each dot depicts the signal intensity of one miRNA, exemplified by the red dot and arrows. The pEV were extracted by sucrose gradient from 24 ml of pooled plasma (4 individuals, 6ml each). AFI: Average fold-increase of all miRNAs over reference. RLU: relative light units. (**B**) Hierarchical clustering based on Euclidean distance of miRNAs extracted from pEV (14ml plasma) from 8 healthy individuals and 2 viremic ($2.1x10^4$ and $5.6x10^3$ viral copies/ ml) and 2 non-viremic HIV-infected individuals. nvir.: non-viremic. vir.: viremic. (**C**) Protein levels (μg) in sucrose gradient fractions 1.13-1.23 (as in Figure 1D) from viremic- (10^3-10^5 viral copy numbers/ml) and non-viremic patients (<20 viral copies/ml) as well as controls (n=4). (**D-E**) Particle number and size analysis of pEV. (**D**) Example of a pEV analysis from a pool of non-viremic individuals and healthy controls (n=4, pools of 24 ml each), subjected to a concentration analysis by dynamic light scattering using a ZetaView® nanoparticle tracker (ParticleMetrix GmbH; Meerbusch, Germany). (**E**) Gradient-purified pEV derived from 15 ml plasma from 7 non-viremic individuals and 6 healthy controls using the ZetaView® nanoparticle tracker. Based on the measurements a pEV concentration per ml plasma was calculated as indicated.

Figure 2: HIV pEV contain viral accessory proteins and inflammatory effectors

(**A**) Western blot analysis of individual sucrose gradient fractions from viremic and non-viremic patients. Purified pEV from samples analyzed in Fig. 1D and viremic patients (n=4, pools of 24 ml each) were blotted for indicated factors. Red arrows in the boxes depict the positive correlation of Nef with ADAM17 and pro-TNF cleavage. precrs.: precursor. **Note**: CD63 and CD81 western blot panels in Fig. 1D and 2A are identical (same samples). Lysates of 293T cells, transfected with p24 Gag (+Gag) and/or Nef/Nef-cofactors (Lys.), served as controls (Cont.). (**B**) Protein array analyzing the content of cytokines, chemokines and soluble factors (CCF) in pEV from healthy controls, viremic patients with low CD4 counts (120-250/μl) and non-viremic HIV patients with high CD4 counts (>750/μl) (30ml pooled plasma, 5 patients). See full CCF list analyzed in supplementary information.

Figure 3: HIV pEV constitute a pEV subclass induced by αvβ3 activation

(**A**) HIV pEV isolation from plasma of 3 non-viremic patients with high or low CD4 count using 2H4-coupled magnetic beads (see Fig. S2). Bead isolated pEV (bead) and flow through (FT) were analyzed for the indicated markers. The lower panel includes an additional control for non-coupled beads, indicated by a sphere w/wo antibody. Red and green boxes point to differences between bead-isolation and FT (details in text). (**B**) CCF protein array analysis of purified pEV

from non-viremic patients (30 ml pooled plasma, 4 patients) coupled to 2H4-coupled beads (beads) and flow through (FT). (**C**) Same experimental set up as in (A). pEV were isolated from two non-viremic patients using 2H4-coupled beads and blotted for indicated markers. Red boxes refer to differences in bead-isolated fraction and flow through as described in the text. (**D**) Expression of Nef and co-factors in 293T cells as indicated and similar as performed previously (Lee et al., 2013), and immunoblot for phosphorylated endogenous Pyk2 and PLCγ. Insert*: longer exposure of negative control and PMA stimulation as compared to the rest of the blot.

Figure 4: Peripheral mononuclear cells ingest large amounts of HIV pEV.
Immunohistochemistry analysis of Nef, Vpu and p24 Gag in plastic adherent PBMC, obtained from non-viremic patients and a healthy controls. (**A**) One representative sample is shown. (**B**) Nef, Vpu and Gag staining as in (A) after incubation of non-viremic HIV pEV (gradient-purified) with plastic-adherent PBMC from a healthy individual. (**C**) Average number of positive cells (in %) stained as in (A) in 4 non-viremic patients. For each patient $3.0x10^2$ cells were analyzed and the mean value was taken as a representative number. (**D**) Western blot analysis of plastic adherent cells from one non-viremic individual (nvir.) and one healthy control (hlt.) for factors as indicated. Nef/co-factors-transfected cells 293T cells (as in Fig. 3E) served as positive control.

Figure 5: $CD1c^+CD14^+$ mononuclear cells contain Nef and secrete inflammatory cytokines.
FACS and immunohistochemistry analysis of Nef-containing mononuclear cells. (**A**) Assessment of $CD1c^+CD14^+$ cells in $CD1c^+$ positive selected PBMC from 2 non-viremic patients and a healthy control. Aliquots of the cells were stained for Nef and CD14 by immunohistochemistry. (**B**) Percentage of $CD1c^+CD14^+$ cells in the $CD1c^+CD19^-$ cell fraction based on the analysis of 5 non-viremic patients and healthy controls. Error bars represent mean ± SEM. (**C**) Secretion of TNF, IL-6 and IFN by 10^5 PBMC obtained from 4 non-viremic patients and controls in 12 hours. PBMC were left untreated or the $CD1c^+$ fraction was positive depleted (by magnetic beads) (**D**) TNF and IL-6 secretion from PBMC, or from 10^5 positive-selected $CD14^+$ and $CD19^+$ cells in 12 h. Error bars show the SEM.

Figure 6: pEV-derived Nef and ADAM17 activity correlate with low T cell counts
(**A**) Correlation of pEV protein levels of Nef and other markers with CD4 count (left panel, arrows) and viral copy numbers (right panel, arrows). Plasma-EV were purified by differential centrifugation from non-viremic and viremic patients. The equivalent of 3 ml plasma was analyzed by Western blot. Lysates (Lys.) of 293T cells, transfected with p24 Gag (Gag Lys.) or Nef/Nef-cofactors (+cont.), served as controls, as well as EV purified from these transfected cells (EV). (**B**) Correlation and significance analyses (Pearsons correlation coefficient (PCC); Students t-test) of pEV-derived Nef-, ADAM17- and p24 Gag-levels with CD4-, CD8-count and

viral copy numbers. Protein-levels were assessed from 16 viremic and 17 non-viremic patients (see Fig. S3 and S4) by Western blot and quantified by ImageJ. Boxes were colored to simplify their explanation in the text. (**C**) Correlation of ADAM17 activity with CD4 count. Plasma EV were purified from 6 viremic and non-viremic patients and 3 healthy controls (left panel), and from 30 ml of pooled plasma (5 patients, 6 ml each), collected from non-viremic HIV patients with different CD4 counts as depicted. Aliquots corresponding to 1 ml of plasma were analyzed using a commercial assay (AnaSpec).

Figure 7: PBMC-derived CCF contribute to HIV pEV

Protein array analyzing the content of cytokines, chemokines and soluble factors (CCF) in EV purified from culture supernatants of Jurkat T cells transfected with a HIV-Δenv construct for 72 hours or vector control (expression control in Fig. S6B), and from resting PBMC from 7 non-viremic individuals and 7 healthy controls cultured separately for 48 hours. For comparison, pEV were purified from plasma pools of viremic/non-viremic patients as described in Fig. 2B. See full CCF list analyzed in supplementary information. Assay input details are summarized in Table S2.

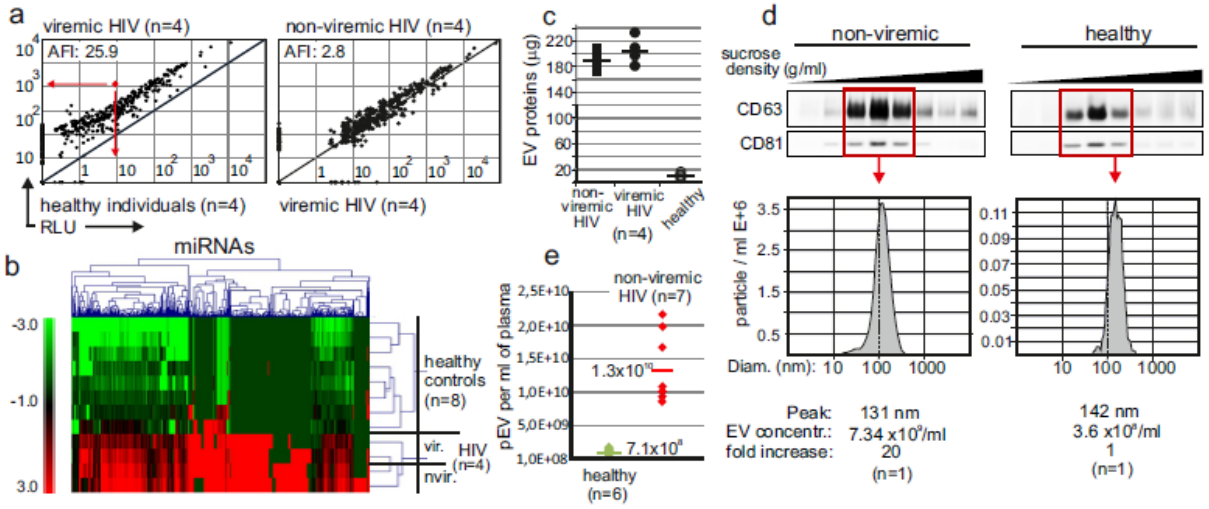

Figure 1

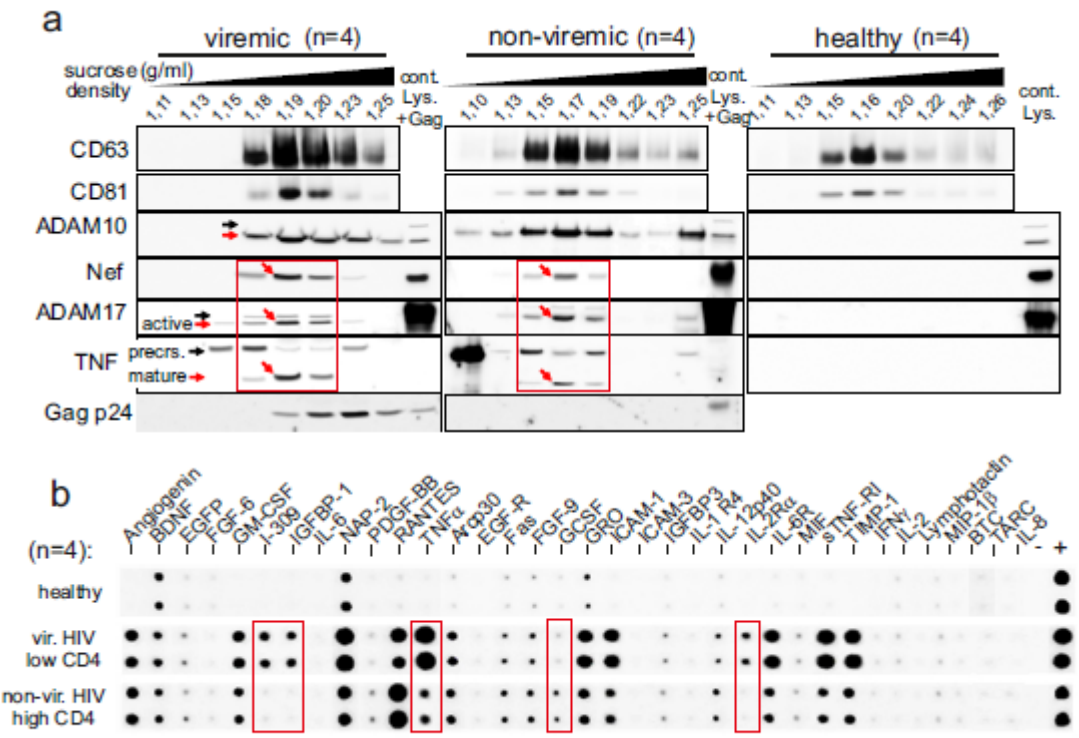

Figure 2

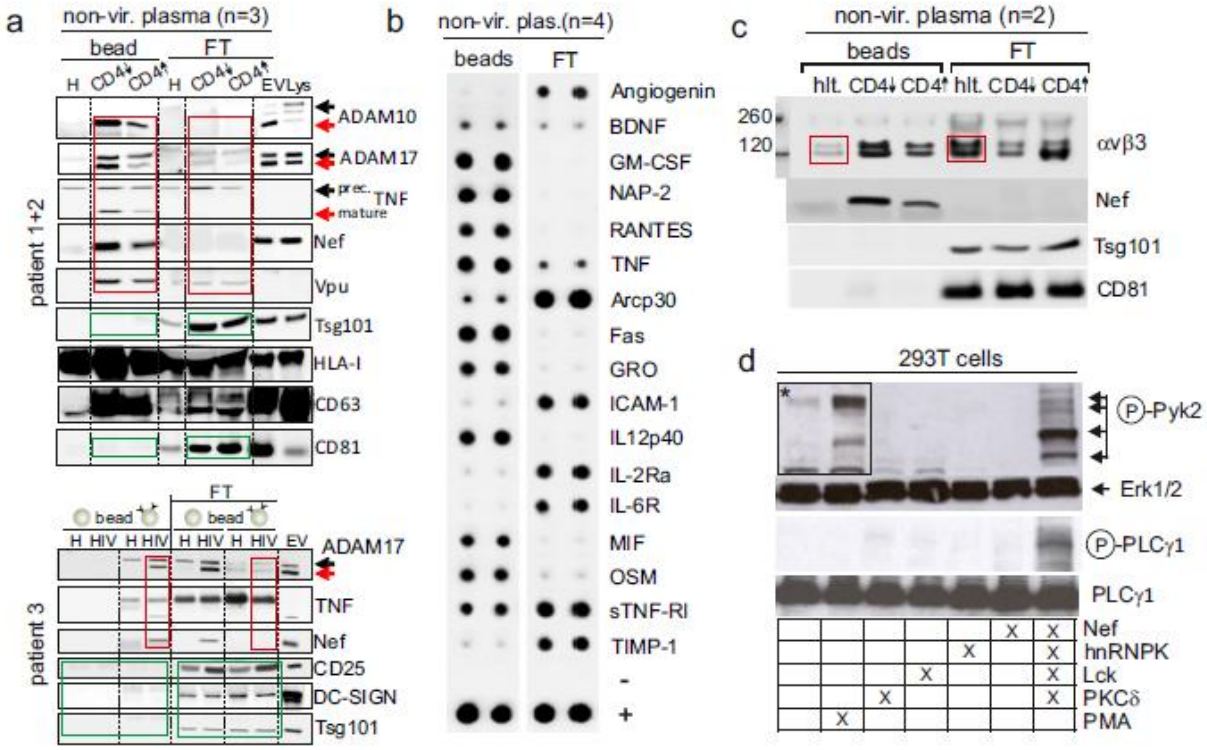

Figure 3

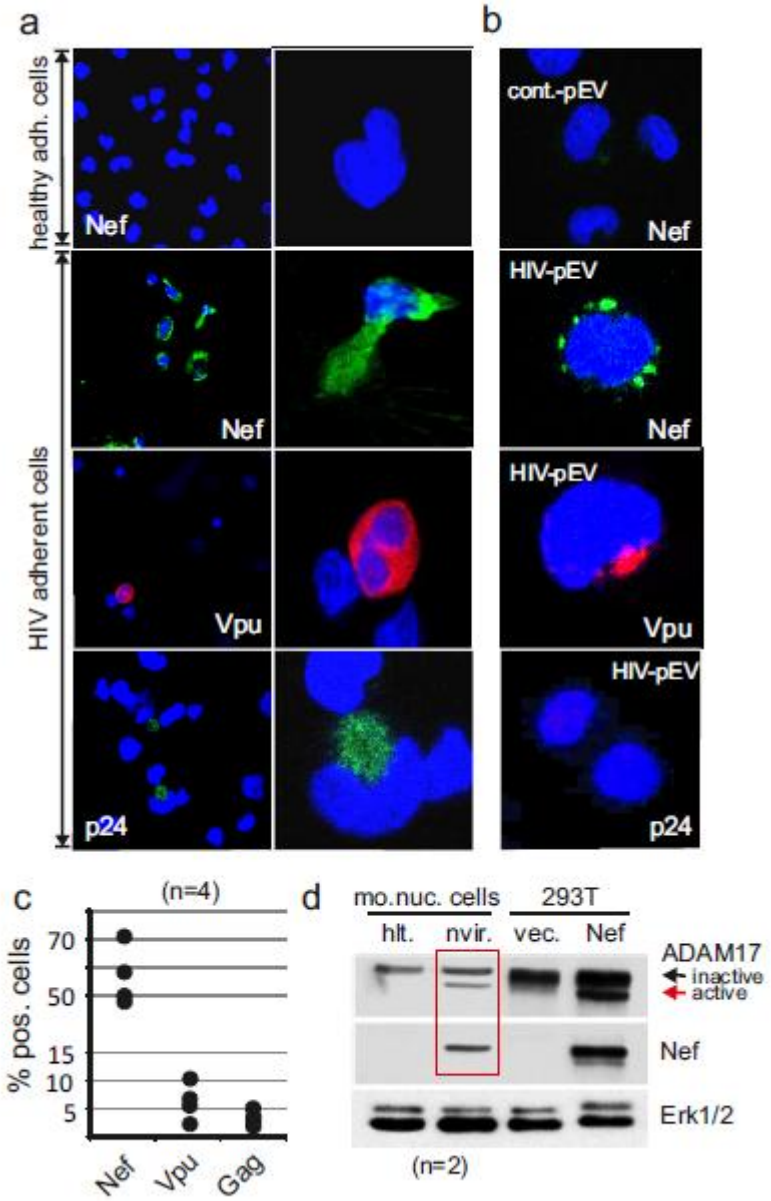

Figure 4

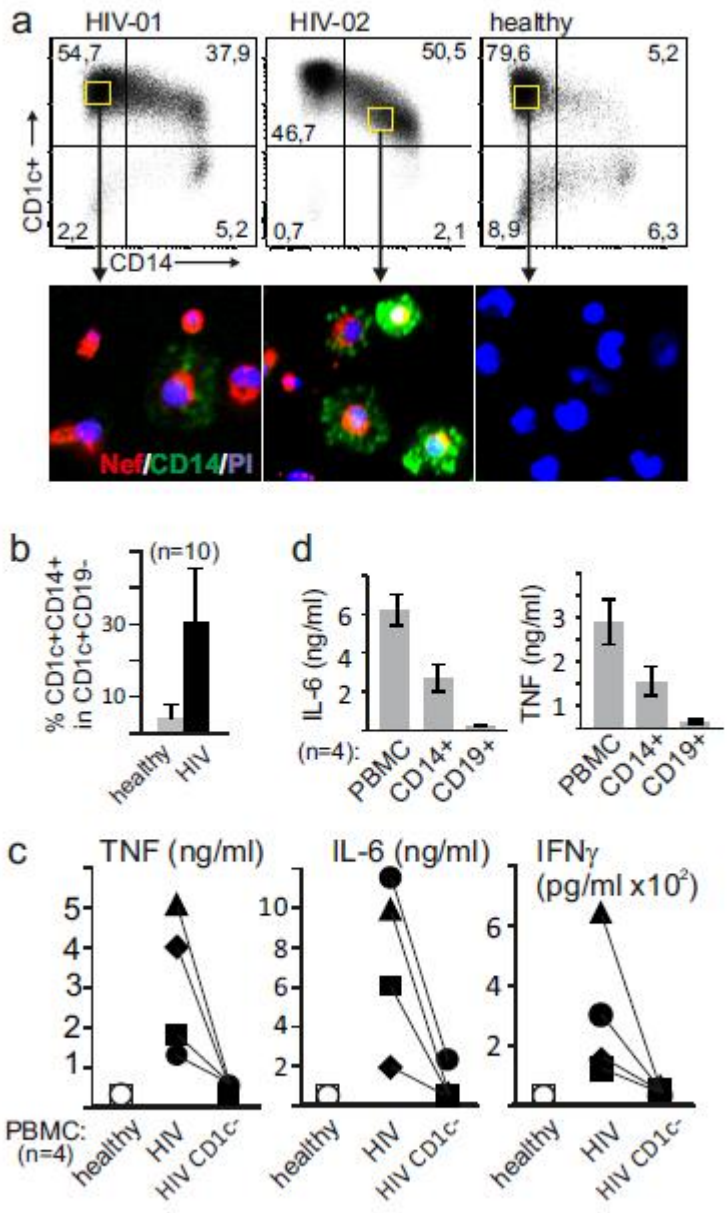

Figure 5

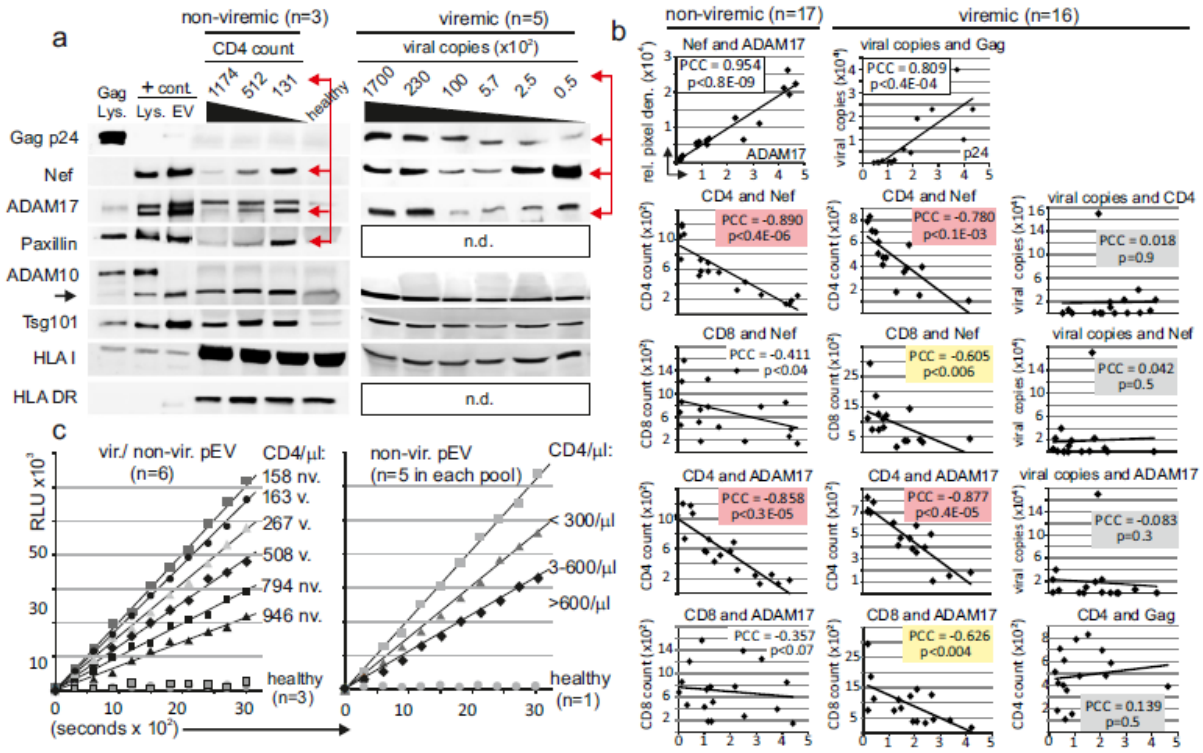

Figure 6

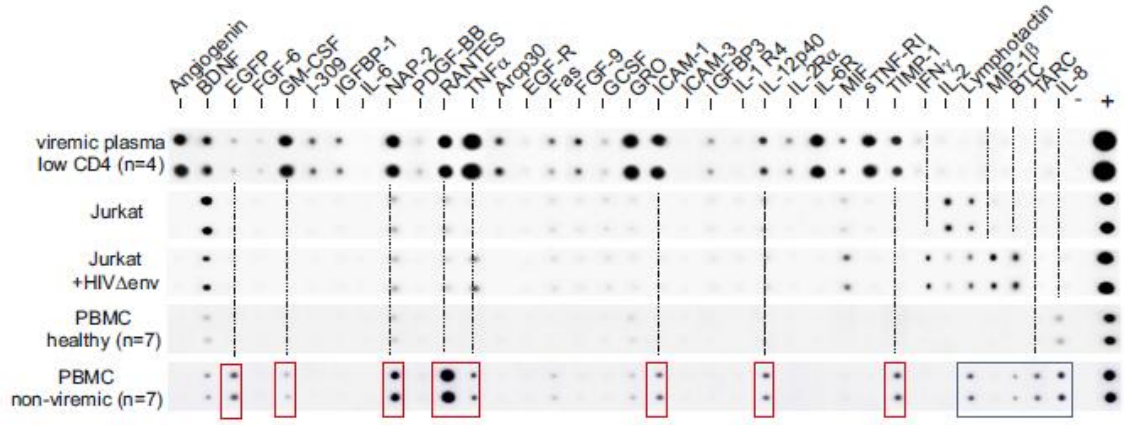

Figure 7